J Sol-Gel Sci Technol (2017) 83:12–18
DOI 10.1007/s10971-017-4372-5

ORIGINAL PAPER: DEVICES BASED ON SOL-GEL OR HYBRID MATERIALS

Influences of sintering temperatures and crystallite sizes on electrochemical properties of $LiNiPO_4$ as cathode materials via sol–gel route for lithium ion batteries

K. Rajammal[1] · D. Sivakumar[2] · Navaneethan Duraisamy[3] · K. Ramesh[1] · S. Ramesh[1]

Received: 21 December 2016 / Accepted: 24 March 2017 / Published online: 22 April 2017

Abstract Acetates of lithium ($LiC_2H_3O_2$) and nickel ($NiC_2H_3O_2$) together with ammonium dihydrogen phosphate $(NH_4)H_2PO_4$ were used as starting materials to prepare $LiNiPO_4$ cathode materials via sol–gel technique. This simple and effective method of using distilled water as main solvent was assisted by small amount of oxalic acid. Final product was obtained after sintering process at temperatures of 500 °C, 600 °C, 700 °C, and 800 °C for 3 h. The peaks in X-ray diffraction patterns reveal ordered olivine structure of $LiNiPO_4$ under Pnma space group. The surface morphologies as in field emission scanning electron microscopy images clearly showed complete formation of $LiNiPO_4$ with uniform size distribution. Charge–discharge tests recorded initial discharge capacities of 97.3 mAh g^{-1} and 91.1 mAh g^{-1} for $LiNiPO_4$ obtained at sintering temperatures of 700 and 800 °C respectively in the voltage range 2.5–4.5 V. Insitu carbon coating during synthesis improved electrochemical performances of $LiNiPO_4$. Sintering temperature 700 °C produced smaller $LiNiPO_4$ particles compared to 800 °C, which enables good capacity retention.

Graphical Abstract

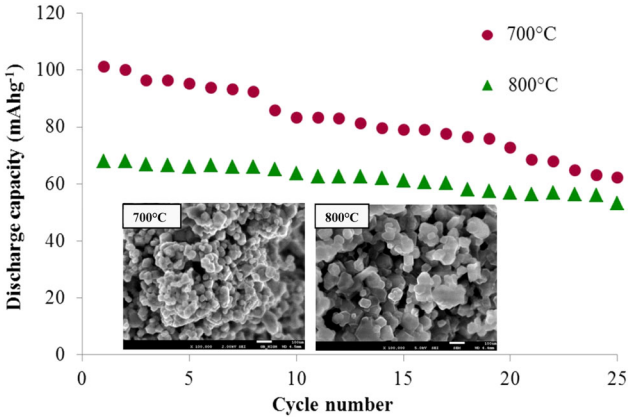

Keywords Olivine · Cathode materials · Sol–gel method · Oxalic acid · Electrochemical analysis

1 Introduction

Lithium ion batteries have dominated as main power source option for portable electronic devices and electric vehicles. New, unique and improved cathode materials are continuously developed as cathode materials are the highly responsible factor for lithium ion batteries performance. Among them, olivine structured orthophosphates, $LiMPO_4$ (M = Fe, Mn, Co, Ni) have been recognized as one of the suitable cathode materials group for lithium ion batteries with its favorable characteristics such as long cycle life, good thermal stability, environment benignity and safety [1, 2]. Strong $(PO_4)^{3-}$ covalent bonding within the structure

✉ S. Ramesh
rameshtsubra@gmail.com

[1] Department of Physics, Center for Ionics University of Malaya, University of Malaya, Kuala Lumpur 50603, Malaysia

[2] Faculty of Mechanical Engineering, Universiti Teknikal Malaysia Melaka (UTeM), 76100 Durian Tunggal, Malacca, Malaysia

[3] Department of Chemistry, Periyar University, Salem 636011 Tamilnadu, India

enables stability [3, 4]. Turning to the potential voltage, $LiFePO_4$ reaches 3.5 V [5–7], $LiMnPO_4$ around 4.1 V [8–10], while $LiCoPO_4$ and $LiNiPO_4$ rises to 4.8 V [11–13] and 5.1 V accordingly [14, 15]. This clearly points out that $LiNiPO_4$ is in the pathway towards promising cathode materials for high voltage lithium batteries.

Nevertheless, its low electronic conductivity, poor lithium diffusion and electrolyte degradation at higher voltage are the main hurdles of $LiNiPO_4$ to achieve high rate electrochemical performance [16, 17]. Generally, numerous modifications such as particle size control [18, 19], metal ion doping [20–23] metal oxide coating [24–26] and carbon coating [27–29] are suggested by researchers to upsurge the efficiency and electronic conductivity of olivine type materials.

Remarkably, synthesis methods and sintering temperatures plays key roles in carbon layer formation and particles growth [30]. In focusing $LiNiPO_4$ cathode materials, notable approaches such as solid state reaction [3, 31], pechini-type polymerizable precursor method [32] and polyol method [15] have been developed for synthesis process. Stefan et al. have synthesized $LiNiPO_4$ and its derivatives $LiNi_{1-y}Co_yPO_4$ ($y = 0.25, 0.33, 0.66, 1.0$) via non aqueous sol–gel route employing ethylene glycol [33]. Capacity about ~ 22 mAh g^{-1} was reported for $LiNiPO_4$. Gangulibabu et al. have produced $LiNiPO_4$ via citric acid assisted sol–gel method. This work reported on structural characterizations, cyclic voltammetry, and electrochemical impedance studies, no electrochemical charge–discharge included. In another work, $LiNiPO_4$ and copper doped $LiNiPO_4$ cathode materials were prepared by microwave assisted non aqueous sol–gel route [34]. The electrocatalytic activities of the samples were evaluated by cyclic voltammetry studies and no electrochemical tests performed. Dimesso et al. have produced $LiNi_{1-y}Mg_yPO_4$ ($0 \leq y \leq 0.3$) using Pechini assisted sol–gel process [35]. $LiNiPO_4$ in this work exhibits initial discharge capacity of 86 mAh g^{-1} at 0.1 C and it showed capacity fade about 8% at the 10th cycle. A Ornek and co-workers have synthesized pristine $LiNiPO_4$ and Co doped $LiNi_{1-x}Co_xPO_4$ ($x = 0.2, 0.4, 0.6, 0.8, 1.0$) by sol–gel technique utilizing citric acid [36]. $LiNiPO_4$ and $LiNiPO_4$-C samples achieved initial discharge capacity of 18 mAh g^{-1} and 86 mAh g^{-1}, respectively.

To the best of our knowledge, even though sol–gel technique has been approached to synthesize $LiNiPO_4$ cathode materials but oxalic acid has not been used as carbon source. Simultaneously, fundamental properties such as effect of sintering temperatures and crystallite size of $LiNiPO_4$ cathode materials have not been studied comprehensively. Considering aforementioned facts, $LiNiPO_4$ is synthesized via oxalic acid assisted sol–gel route in this work. Sol–gel route signifies a versatile technique for cathode materials due to its high molecular level mixing, thus widely employed to produce olivines [37–40]. Oxalic acid serves as both chelating agent and carbon source. It turned to carbon during calcination process, thus coated the particles and improve the conductivity of the samples [41, 42]. It also provides high level reactants mixing which yields good product with enhanced performance [43]. Hence, this work will draw insights on influences of sintering temperatures and crystallite size on electrochemical properties of $LiNiPO_4$ cathode materials.

2 Experimental

Stoichiometric amounts of 0.2 m (20.404 g) lithium acetate ($LiC_2H_3O_2$) (Aldrich), 0.2 m (49.768 g) nickel acetate Ni $(CH_3COO)_2{\cdot}4H_2O$ (Friendmann Schmidt) and 0.2 m (23.006 g) ammonium dihydrogen phosphate $(NH_4)H_2PO_4$ (Friendmann Schmidt) were dissolved in 500 mL distilled water under continuous magnetic stirring and heating. 10 wt.% of oxalic acid was added to the solution. The solution was continuously stirred and heated (120 °C) about 4 h until solid precursor formed. The precursor was ground and then calcined at 500 °C, 600, 700, and 800 °C for 3 h. The samples were ground again after the calcination for further structural characterizations.

Crystalline phases of the samples were obtained by X-ray diffraction (XRD) using Siemens D 5000 diffractometer equipped with Cu–Kα radiation ($\lambda = 1.54060$ Å). Morphological phases were acquired by field emission scanning electron microscope (FESEM, model JSM 7600-F). Raman spectra were collected from Raman spectrometer (In-via Raman microscope) using wavelength of 532 nm (blue laser).

Electrochemical properties were evaluated by coin cells consist of cathode, lithium metal anode and 1 M $LiPF_6$ dissolved in a mixture of ethylene carbonate/ dimethyl carbonate (1:1 in volume) electrolyte. The cathode was prepared by mixing 62.5% $LiNiPO_4$, 25% teflonized acetyle black, 12.5% graphite and coated on the stainless steel mesh. The coin cells were fabricated in Argon filled glove box. Cycling tests were carried out at current rate of 0.02C (1C=171 mAh g^{-1}) between 2.5 and 4.5 V in a Neware battery system.

3 Results and discussion

XRD patterns of $LiNiPO_4$ materials heat treated at different temperatures are shown in Fig. 1. All the intense peaks in the diagram clearly indicate orthorhombic olivine structure of $LiNiPO_4$ with Pnma space group and good agreement with JCPDS no. 81-1528 [15]. Diffraction peaks of (101), (111), (020), (311), and (121) can be seen at $2\theta = 20.9°$,

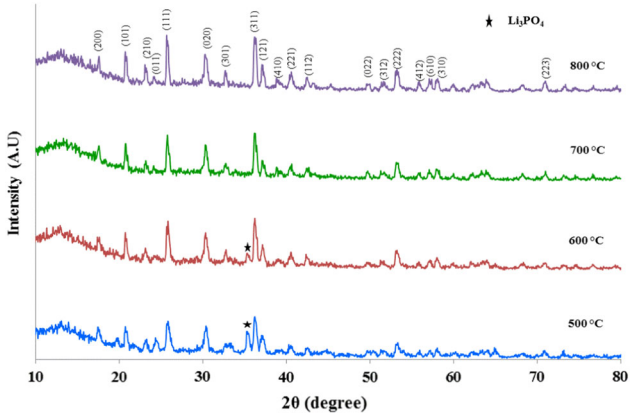

Fig. 1 XRD pattern of $LiNiPO_4$ at different sintering temperatures

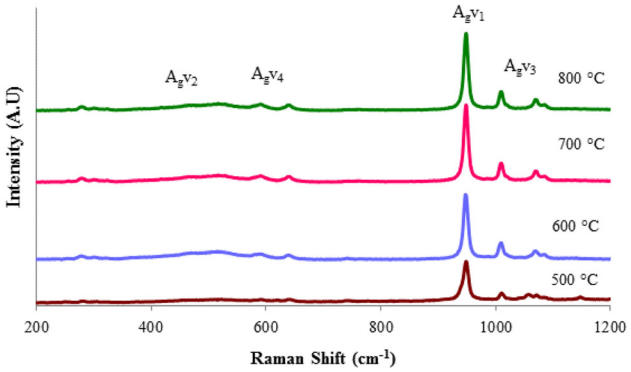

Fig. 2 Raman spectra of $LiNiPO_4$ at different heating temperatures

25.9°, 30.5° 36.4°, and 37.3°, respectively. $LiNiPO_4$ crystallized completely at low sintering temperatures of 500 and 600 °C by oxalic acid assisted sol–gel synthesis even though there is impurity peak which corresponds to Li_3PO_4 [3]. It also can be noticed that Li_3PO_4 impurity diminished at higher calcination temperature of 700 and 800 °C which forms pure phase of $LiNiPO_4$.

As the calcination temperature increases, the characteristic peaks getting sharper evidently explain that the improved crystallinity achieved at higher temperatures [44]. No obvious diffraction peaks related to residual carbon indicating that carbon amount is low and in amorphous state [45, 46].

Raman spectra as in Fig. 2 presenting dominant band at 948 cm^{-1} in $LiNiPO_4$ assigned to symmetric A_gv_1 mode. The peaks located at 1011 cm^{-1} and 1082 cm^{-1} denote asymmetric stretching vibration of PO_4 tetrahedron. The peak at 290 cm^{-1} represents asymmetric stretching vibration of Li–O bonds. While the broad peak at 478 cm^{-1} fits to symmetric A_gv_2 mode. The other peaks at 597 and 649 cm^{-1} indicates symmetric A_gv_4 modes [32, 47].

The surface morphologies and particle sizes of $LiNiPO_4$ obtained at various calcination temperatures were examined by FESEM and the images are illustrated in Fig. 3. Well-crystallized polyhedral particles are formed with smooth surfaces at all the calcination temperatures. The particles present with less agglomeration and there is no much variation in the particles shape. The particles are within the range of 100–150 nm at the sintering temperatures of 500, 600, and 700 °C. At the sintering temperature of 800 °C, particles are in the size of 100–200 nm.

Uniform size distribution of $LiNiPO_4$ achieved with the aid of oxalic acid which served as organic fuel during calcination process. Large amount of gas released during oxalate decomposition. Thus, it suppressed agglomeration of particles [48, 49]. Wang et al. [50] have highlighted that chelating agents in sol gel technique able to provide high molecular level mixing, thus results in pure phase structure and morphology.

Fig. 4 depicting the Williamson–Hall plots of $\beta \cos \theta$ vs. $\sin \theta$ for $LiNiPO_4$ samples calcined at different temperatures from 500 to 800 °C. The slope of the graph represents strain value and the line interception provides inverse crystallite size value [51, 52].

The crystallite size deduced from the graph increases with sintering temperature, this also proved by XRD peaks which getting sharper with rise of heating temperature [53]. At 500 and 600 °C, the crystallite size of $LiNiPO_4$ is 24.8 and 26.2 nm respectively. $LiNiPO_4$ attained at calcination temperature 700 °C has crystallites in the range of 28.9 nm while at sintering temperature of 800 °C contain crystallite sizes of 29.5 nm. Even though, the crystallites sizes seem like moreover within similar range, different strain values are signifying crystal defects that present within the particles [51]. Sintering temperatures of 500 °C and 600 °C recorded the strain values of 2.75×10^{-4} and 1.25×10^{-4} correspondingly. Strain value of crystallites that produced at heating temperature of 700 °C is 5.0×10^{-5}, whereas the strain value increased to 2.0×10^{-4} for the sample that obtained at 800 °C. From the results, it can be concluded that $LiNiPO_4$ obtained at sintering temperature of 700 °C has the smallest strain value. Higher strain value for the samples sintered at 500 and 600 °C maybe attributed to impurities that present in the samples as depicted in XRD results. Moreover, high strain value for the samples sintered at 800 °C could be due to the instability of structure formed at high temperature.

Present work demonstrates that cathode materials produced at sintering temperature of 700 °C and 800 °C have good structural properties without any impurities. Hence, these samples were chosen for electrochemical testing. Figure 5 displays first and twenty-fifth charge–discharge curves of $LiNiPO_4$ at a current rate of 0.02 C.

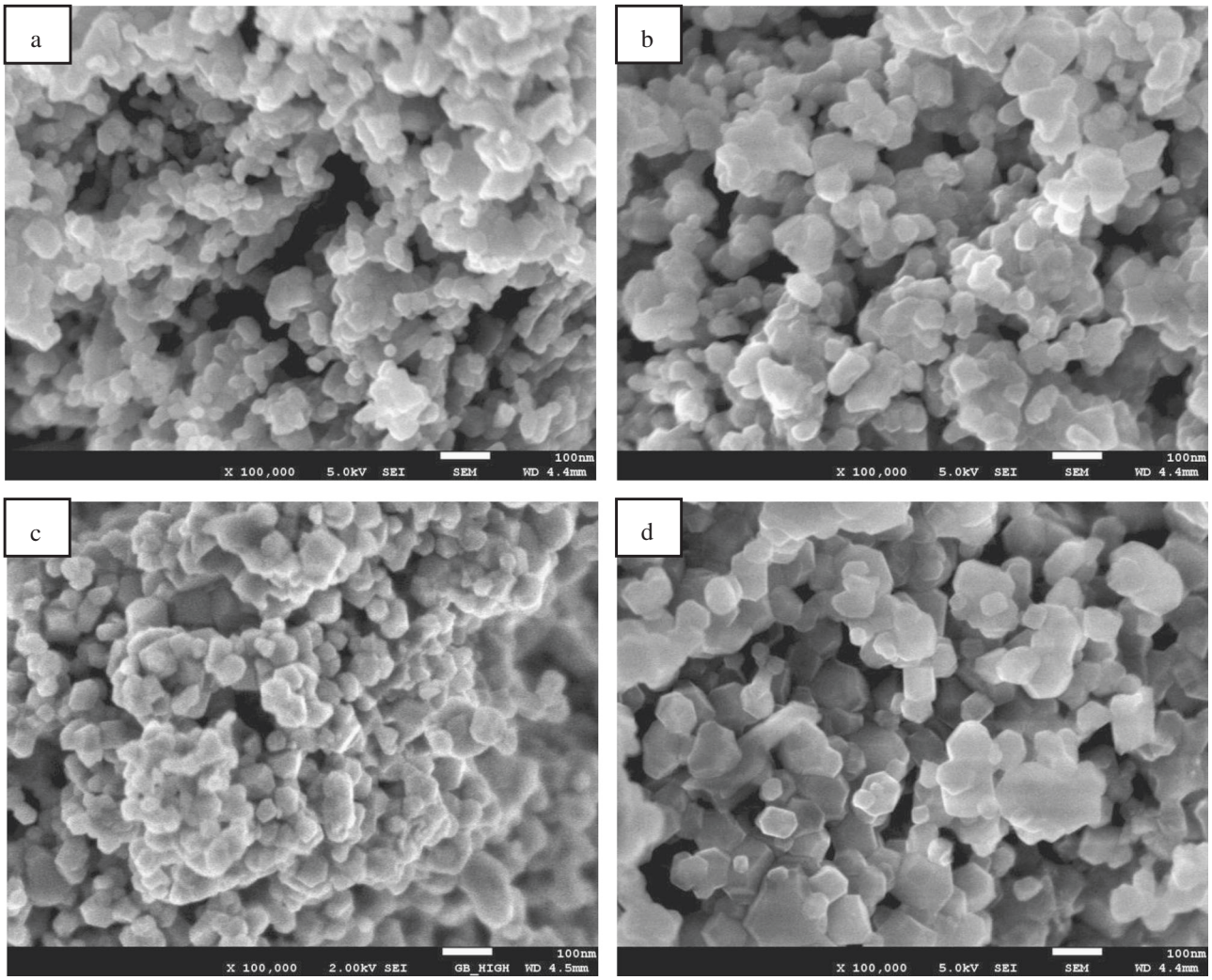

Fig. 3 FESEM micrographs of $LiNiPO_4$ obtained at (**a**) 500 °C (**b**) 600 °C (**c**) 700 °C (**d**) 800 °C

Initial charge and discharge capacities of $LiNiPO_4$ obtained at heating temperature of 700 °C were 97.7 mAh g^{-1} and 97.3 mAh g^{-1}, respectively. Hence, initial cycle performance records high coulombic efficiency value of 97.1% with irreversible capacity loss around 0.4 mAh g^{-1}. While $LiNiPO_4$ produced at calcination temperature of 800 °C exhibited initial charge capacity about 93.7 mAh g^{-1} and discharge capacity of 91.1 mAh g^{-1} corresponds to 97.2% coulombic efficiency with irreversible capacity loss 2.6 mAh g^{-1}.

Figure 6 summarizes electrochemical performances of both samples in the voltage range of 2.5 and 4.5 V. It can be observed that discharge capacity of $LiNiPO_4$ processed at calcination temperature of 700 °C higher than 800 °C.

In situ carbon coating aided by oxalic acid in synthesis process shows notable enhancement to the first discharge capacity of both samples compared to literature [35, 36]. Among the both samples, $LiNiPO_4$ obtained at calcination temperature 700 °C demonstrates better electrochemical performance than 800 °C, can be accredited to the smaller crystallites. When the crystallite size is reduced, it offer more contact area to electrolyte. It is also beneficial to diminish structural degradation during charging and discharging process [54]. Besides that, shortened electron and lithium ion diffusion paths lead to the enhanced electrochemical properties [55–57]. On contrary, higher strain in sample that obtained at heating temperature of 800 °C impedes smooth lithium intercalation and deintercalation [58, 59]. At the same time, crystal defects that formed at higher sintering temperature affect the cycling performance. It can be concluded that sintering temperatures during synthesis process indirectly influences crystallite size of the samples [60]. Thus, sintering temperature can be optimized to control the size of the crystallites and strain of the particles.

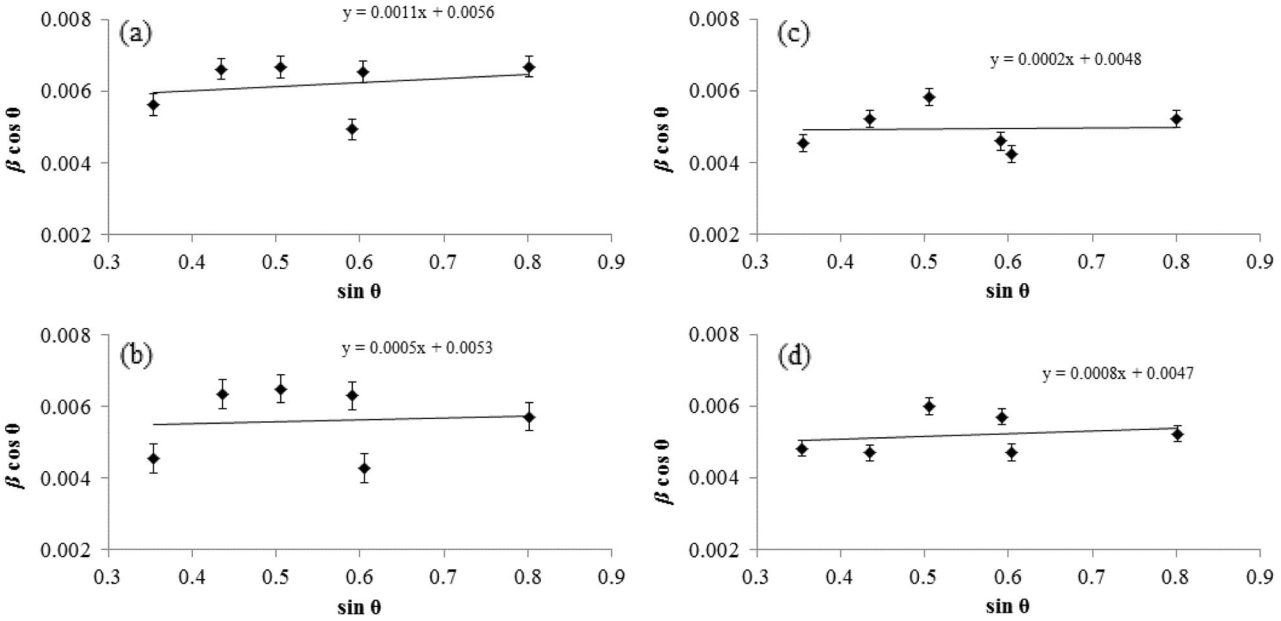

Fig. 4 Williamson-hall plots of $LiNiPO_4$ produced at sintering temperature of (**a**) 500 °C (**b**) 600 °C (**c**) 700 °C, and (**d**) 800 °C

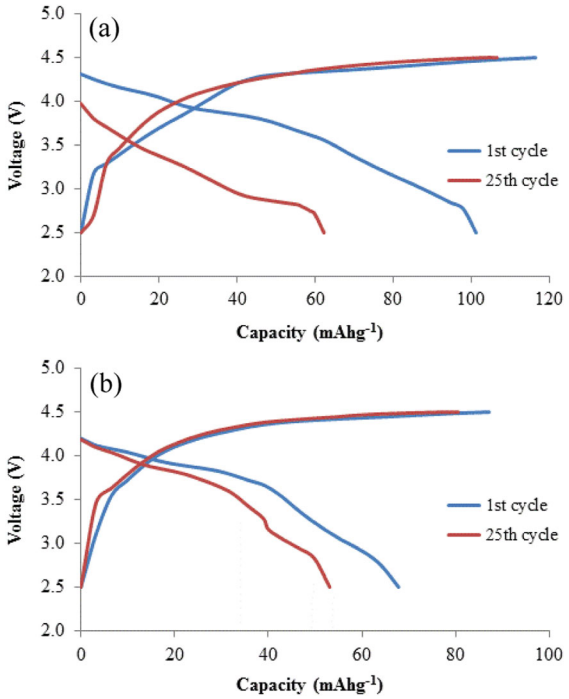

Fig. 5 First and twenty-fifth charge–discharge curves of $LiNiPO_4$ obtained at sintering temperature of (**a**) 700 °C and (**b**) 800 °C

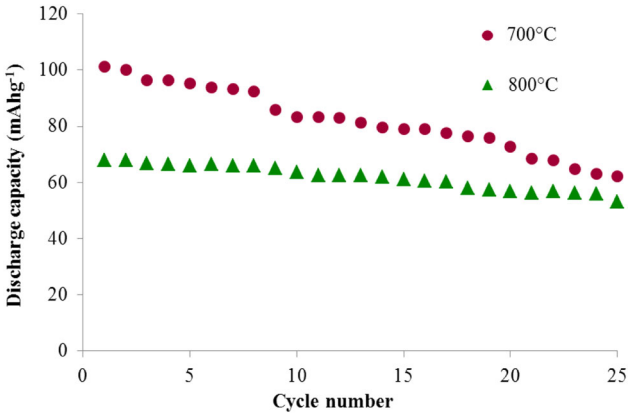

Fig. 6 Charge–discharge behavior of $LiNiPO_4$ obtained at sintering temperature of 700 and 800 °C

4 Conclusion

Olivine type $LiNiPO_4$ cathode materials have been effectively synthesized by oxalic acid aided sol gel route. Oxalic acid is beneficial as chelating agent and carbon source to form in situ carbon coating on $LiNiPO_4$. Samples sintered at 700 and 800 °C, which demonstrates no impurity and good crystallinity employed as cathode materials in lithium half cells. $LiNiPO_4$ obtained at heating temperature 700 °C exhibits initial discharge capacity 97.3 mAh g^{-1} and improved electrochemical performance due to its reduced diffusion path by smaller crystallite size and low strain compared to 800 °C. Sintering temperature can be optimized during sol gel synthesis process for enriched final product.

Acknowledgements Authors would like to thank financial support from the University of Malaya for the PPP grant PG 099—2014B and Fundamental Research Grant Scheme (FP012-2015A), from Ministry of Education, Malaysia. One of the author Dr. Navaneethan Duraisamy acknowledges UGC-Dr. D.S. Kothari Postdoctoral Fellowship (Ref no: No.F.4-2/2006 (BSR)/EN/15-16/0031)

Compliance with Ethical Standards

Conflict of Interest The authors declare that they have no competing of interest.

References

1. Rui X, Zhao X, Lu Z, Tan H, Sim D, Hng HH et al. (2013) Olivine-Type Nanosheets for Lithium Ion Battery Cathodes, ACS Nano 7(6):5637–5646
2. Alyoshin VA, Pleshakov EA, Ehrenberg H, Mikhailova D (2014) Platelike $LiMPO_4$ (M=Fe, Mn, Co, Ni) for Possible Application in Rechargeable Li Ion Batteries: beyond Nanosize. J Phys Chem C 4:17426–17435
3. Minakshi M, Singh P, Appadoo D, Martin DE (2011) Synthesis and characterization of olivine $LiNiPO_4$ for aqueous rechargeable battery. Electrochim Acta 56:4356–4360
4. Chen H, Chen M, Du C, Cui Y, Zuo P (2016) Synthesis and electrochemical performance of hierarchical nanocomposite of carbon coated $LiCoPO_4$ crosslinked by graphene. Mater Chem Phys 171:6–10
5. Gong C, Xue Z, Wen S, Ye Y, Xie X (2016) Advanced carbon materials/olivine $LiFePO_4$ composites cathode for lithium ion batteries. J Power Sources 318:93–112
6. Zhang SM, Zhang JX, Xu SJ, Yuan XJ, He BC (2013) Li ion diffusivity and electrochemical properties of $FePO_4$ nanoparticles acted directly as cathode materials in lithium ion rechargeable batteries. Electrochim Acta 88:287–293
7. Zhang Y, Huo Q, Du P, Wang L, Zhang A, Song Y et al. (2012) Advances in new cathode material $LiFePO_4$ for lithium-ion batteries. Synth Met 162:1315–1326
8. Huang Q, Wu Z, Su J, Long Y, Lv X, Wen Y (2016) Synthesis and electrochemical performance of Ti – Fe co-doped $LiMnPO_4$/C as cathode material for lithium-ion batteries. Ceram Int 42:11348–11354
9. Xiong J, Wang Y, Wang Y, Zhang J (2016) PVP-assisted solvothermal synthesis of $LiMn_{0.8}Fe_{0.2}PO_4$/C cathode material for lithium ion batteries. Ceram Int 42:9018–9024
10. Ding J, Su Z, Tian H (2016) Synthesis of high rate performance $LiFe_{1-x}Mn_xPO_4$/C composites for lithium-ion batteries. Ceram Int 42:12435–12440
11. Karthickprabhu S, Hirankumar G, Maheswaran A, Bella RSD, Sanjeeviraja C (2014) Structural and electrical studies on Zn^{2+} doped $LiCoPO_4$. J Electrostat 72:181–186
12. Li H, Wang Y, Yang X, Liu L, Chen L, Wei J (2014) Improved electrochemical performance of 5 V $LiCoPO_4$ cathode materials via yttrium doping. Solid State Ionics 255:84–88
13. Doan TNL, Taniguchi I (2012) Effect of spray pyrolysis temperature on physical and electrochemical properties of $LiCoPO_4$/C nanocomposites. Powder Technol 217:574–580
14. Truong QD, Devaraju MK, Honma I (2014) $LiMPO_4$ nanoplates by a supercritical ethanol. J Mater Chem A Mater Energy Sustain 2:17400–17407
15. Karthickprabhu S, Hirankumar G, Maheswaran A, Sanjeeviraja C, Bella RSD (2013) Structural and conductivity studies on $LiNiPO_4$ synthesized by the polyol method. J Alloys Compd 548:65–69
16. Örnek A, Kazancioglu MZ (2016) A novel and effective strategy for producing core-shell $LiNiPO_4$/C cathode material for excellent electrochemical stability using a long-time and low-level microwave approach. Scr Mater 122:45–49
17. Devaraju MK, Truong QD, Honma I (2015) One pot synthesis of in situ Au decorated LiNiPO4 nanoplates for Li-ion batteries, Applied Materialstoday 1:95–99
18. Hamamoto K, Fukushima M, Mamiya M, Yoshizawa Y, Akimoto J, Suzuki T et al. (2012) Morphology control and electrochemical properties of $LiFePO_4$/C composite cathode for lithium ion batteries. Solid State Ionics 225:560–563
19. Yoshida J, Stark M, Holzbock J, Hüsing N, Nakanishi S, Iba H et al. (2013) Analysis of the size effect of $LiMnPO_4$ particles on the battery properties by using STEM-EELS. J Power Sources 226:122–126
20. Zhao RR, Hung IM, Li YT, Chen HY, Lin CP (2012) Synthesis and properties of Co-doped LiFePO 4 as cathode material via a hydrothermal route for lithium-ion batteries. J Alloys Compd 513:282–288
21. Fang H, Yi H, Hu C, Yang B, Yao Y, Ma W (2012) Effect of Zn doping on the performance of $LiMnPO_4$ cathode for lithium ion batteries. Electrochim Acta 71:266–269
22. Hu C, Yi H, Fang H, Yang B, Yao Y, Ma W et al. (2010) Improving the electrochemical activity of $LiMnPO_4$ via Mn-site co-substitution with Fe and Mg. Electrochem commun 12:1784–1787
23. Rajammal K, Sivakumar D, Duraisamy N, Ramesh K, Ramesh S (2016) Structural and electrochemical characterizations of $LiMn_{1-x}Al_{0.5x}Cu_{0.5x}PO_4$ (x=0.0, 0.1, 0.2) cathode materials for lithium ion batteries. Mater Lett 173:131–135
24. Lee J, Kumar P, Lee J, Moudgil BM, Singh RK (2013) ZnO incorporated $LiFePO_4$ for high rate electrochemical performance in lithium ion rechargeable batteries. J Alloys Compd 550:536–544
25. Li Y-D, Zhao S-X, Nan C-W, Li B-H (2011) Electrochemical performance of SiO_2-coated $LiFePO_4$ cathode materials for lithium ion battery. J Alloys Compd 509:957–960
26. Rajammal K, Sivakumar D, Duraisamy N, Ramesh K, Ramesh S, (2016) Enhanced electrochemical properties of ZnO-coated LiMnPO4 cathode materials for lithium ion batteries, Ionics (Kiel) 22:1551–1556
27. Zhao D, Feng Y, Wang Y, Xia Y (2013) Electrochemical performance comparison of $LiFePO_4$ supported by various carbon materials. Electrochim Acta 88:632–638
28. Cheng G, Zuo P, Wang L, Shi W, Ma Y, Du C, Cheng X, Gao Y, Yin G (2015) High-performance carbon-coated LiMnPO4 nanocomposites by facile two-step solid-state synthesis for lithium-ion battery, J Solid State Electr 19:281–288
29. Zhou X, Xie Y, Deng Y, Qin X, Chen G (2015) The enhanced rate performance of $LiFe_{0.5}Mn_{0.5}PO_4$/C cathode material via synergistic strategies of surfactant-assisted solid state method and carbon coating. Mater Chem A 3:996–1004
30. Xie G, Zhu HJ, Liu XM, Yang H (2013) A core-shell $LiFePO_4$/C nanocomposite prepared via a sol-gel method assisted by citric acid. J Alloys Compd 574:155–160
31. Bechir MBEN, Rhaiem ABEN, Guidara K (2014) A. C. conductivity and dielectric study of $LiNiPO_4$ synthesized by solid-state method. Bull Mater Sci 37:1–8
32. Prabu M, Selvasekarapandian S (2012) Dielectric and modulus studies of $LiNiPO_4$. Mater Chem Phys 134:366–370
33. Rommel SM, Rothballer J, Schall N, Brünig C, Weihrich R (2015) Characterization of the carbon-coated $LiNi_{1-y}Co_yPO_4$ solid solution synthesized by a non-aqueous sol-gel route. Ionics 325–333
34. Nucleus T, Umtaz MM, Yaqub A, Bahat SSA, Mujtaba A (2014) Electrocatalytic activity of $LiNiPO_4$ and the copper doped analogues towards oxygen reduction. Nucleus 1:109–115
35. Dimesso L, Spanheimer C, Jaegermann W (2013) Effect of the Mg-substitution on the graphitic carbon foams—$LiNi_{1-y}Mg_yPO_4$ composites as possible cathodes materials for 5 V applications. Mater Res Bull 48:559–565
36 Örnek A, Bulut E, Can M (2015) Influence of gradual cobalt substitution on lithium nickel phosphate nano-scale composites for high voltage applications. Mater Charact 106:152–162

37. Zhao X, Baek D, Manuel J, Heo M, Yang R, Keun J et al. (2012) Electrochemical properties of magnesium doped $LiFePO_4$ cathode material prepared by sol – gel method. Mater Res Bull 47:2819–2822
38. Jiang T, Pan W, Wang J, Bie X, Du F, Wei Y et al. (2010) Carbon coated $Li_3V_2(PO_4)_3$ cathode material prepared by a PVA assisted sol—gel method. Electrochim Acta 55:3864–3869
39. Sheng-kui Z, You W, Jie-qun LIU, Jian W (2012) Synthesis of $LiMnPO_4$/C composite material for lithium ion batteries by sol gel method. Trans Nonferrous Met Soc China 22:2535–2540
40. Manikandan P, Periasamy P, Jagannathan R (2013) Sol-gel synthesis and impedance characteristics of networked nanocrystalline olivine cathode for Li-ion full cells. J Mater Chem A 1:15397–15405
41. Jugović D, Mitrić M, Kuzmanović M, Cvjetićanin N, Škapin S, Cekić B et al. (2011) Preparation of $LiFePO_4$/C composites by co-precipitation in molten stearic acid. J Power Sources 196:4613–4618
42. Kim K, Cho Y, Kam D, Kim H, Lee J (2010) Effects of organic acids as reducing agents in the synthesis of $LiFePO_4$. J Alloys Compd 504:166–170
43. Jian XM, Wenren HQ, Huang S, Shi SJ, Wang XL, Gu CD et al. (2014) Oxalic acid-assisted combustion synthesized $LiVO_3$ cathode material for lithium ion batteries. J Power Sources 246:417–422
44. Kabi S, Ghosh A (2013) Microstructure of Li $(Mn_{1/3}Ni_{1/3}Co_{1/3})O_2$ cathode material for lithium ion battery: Dependence of crystal structure on calcination and heat-treatment temperature. Mater Res Bull 48:3405–3410
45. Lu J, Zhou Y, Jiang T, Tian X, Tu X, Wang P (2016) Synthesis and optimization of three-dimensional lamellar $LiFePO_4$ and nanocarbon composite cathode materials by polyol process. Ceram Int 42:1281–1292
46. Han B, Meng X, Ma L, Nan J (2016) Nitrogen-doped carbon decorated $LiFePO_4$ composite synthesized via a microwave heating route using polydopamine as carbon—nitrogen precursor. Ceram Int 42:2789–2797
47. Ben Bechir M, Ben Rhaiem A, Guidara K (2014) A. C. conductivity and dielectric study of $LiNiPO_4$ synthesized by solid-state method. Bull Mater Sci 37:1–8
48. Wang L, Zhou X, Guo Y (2010) Synthesis and performance of carbon-coated $Li_3V_2(PO_4)_3$ cathode materials by a low temperature solid-state reaction. J Power Sources 195:2844–2850
49. Wei C, He W, Zhang X, Xu F, Liu Q, Sun C et al. (2015) Effects of morphology on the electrochemical performances of $Li_3V_2(PO_4)_3$ cathode material for lithium ion batteries. RSC Adv 5:54225–54245
50. Wang D, Cao L, Huang J, Wu J (2013) Effects of different chelating agents on the composition, morphology and electrochemical properties of LiV_3O_8 crystallites synthesized via sol – gel method. Ceram Int 39:3759–3764
51. Muruganantham R, Sivakumar M, Subadevi R (2015) Enhanced rate performance of multiwalled carbon nanotube encrusted olivine type composite cathode material using polyol technique. J Power Sources 300:496–506
52. Kwon SN, Song J, Mumm DR (2011) Effects of cathode fabrication conditions and cycling on the electrochemical performance of $LiNiO_2$ synthesized by combustion and calcination. Ceram Int 37:1543–1548
53. Zuo R, Liang X, Liu Z (2014) Synthesis and characterization of LiNi1/3Co1/3Mn1/3O2 material for rechargeable lithium batteries by polyacrylic acid-assisted sol – gel method, J Sol–Gel Sci Technol 69:303–310
54. Rommel SM, Schall N, Brünig C, Weihrich R (2014) Challenges in the synthesis of high voltage electrode materials for lithium-ion batteries: a review on $LiNiPO_4$. Monatsh Chem 145:385–404
55. Xiao L, Guo Y, Qu D, Deng B, Liu H, Tang D (2013) Influence of particle sizes and morphologies on the electrochemical performances of spinel $LiMn_2O_4$ cathode materials. J Power Sources 225:286–292
56. Zhu C, Nobuta A, Saito G, Nakatsugawa I, Akiyama T (2014) Solution combustion synthesis of $LiMn_2O_4$ fine powders for lithium ion batteries. Adv Powder Technol 25:342–347
57. Cai Y, Huang Y, Wang X, Jia D, Pang W, Guo Z et al. (2015) Facile synthesis of $LiMn_2O_4$ octahedral nanoparticles as cathode materials for high capacity lithium ion batteries with long cycle life. J Power Sources 278:574–581
58. Liu J, Chen H, Xie J, Sun Z, Wu N, Wu B (2014) Electrochemical performance studies of Li-rich cathode materials with different primary particle sizes. J Power Sources 251:208–214
59. Wang X, Cheng K, Zhang J, Yu L, Yang J (2013) Advanced powder technology effect of carbon content and calcination temperature on the electrochemical performance of lithium iron phosphate/carbon composites as cathode materials for lithium-ion batteries. Adv Powder Technol 24:593–598
60. Rajammal K, Sivakumar D, Duraisamy N, Ramesh K, Ramesh S (2016) Effect of sintering temperature on structural properties of LiMnPO4 cathode materials obtained by sol – gel method. J Sol–Gel Sci Technol 80:514–522